

Evidence for a $B_s^0\pi^\pm$ State

V.M. Abazov,³¹ B. Abbott,⁶⁷ B.S. Acharya,²⁵ M. Adams,⁴⁶ T. Adams,⁴⁴ J.P. Agnew,⁴¹ G.D. Alexeev,³¹ G. Alkhazov,³⁵ A. Alton^a,⁵⁶ A. Askew,⁴⁴ S. Atkins,⁵⁴ K. Augsten,⁷ V. Aushev,³⁸ Y. Aushev,³⁸ C. Avila,⁵ F. Badaud,¹⁰ L. Bagby,⁴⁵ B. Baldin,⁴⁵ D.V. Bandurin,⁷⁴ S. Banerjee,²⁵ E. Barberis,⁵⁵ P. Baringer,⁵³ J.F. Bartlett,⁴⁵ U. Bassler,¹⁵ V. Bazterra,⁴⁶ A. Bean,⁵³ M. Begalli,² L. Bellantoni,⁴⁵ S.B. Beri,²³ G. Bernardi,¹⁴ R. Bernhard,¹⁹ I. Bertram,³⁹ M. Besançon,¹⁵ R. Beuselinck,⁴⁰ P.C. Bhat,⁴⁵ S. Bhatia,⁵⁸ V. Bhatnagar,²³ G. Blazey,⁴⁷ S. Blessing,⁴⁴ K. Bloom,⁵⁹ A. Boehnlein,⁴⁵ D. Boline,⁶⁴ E.E. Boos,³³ G. Borissov,³⁹ M. Borysova^l,³⁸ A. Brandt,⁷¹ O. Brandt,²⁰ M. Brochmann,⁷⁵ R. Brock,⁵⁷ A. Bross,⁴⁵ D. Brown,¹⁴ X.B. Bu,⁴⁵ M. Buehler,⁴⁵ V. Buescher,²¹ V. Bunichev,³³ S. Burdin^b,³⁹ C.P. Buszello,³⁷ E. Camacho-Pérez,²⁸ B.C.K. Casey,⁴⁵ H. Castilla-Valdez,²⁸ S. Caughron,⁵⁷ S. Chakrabarti,⁶⁴ K.M. Chan,⁵¹ A. Chandra,⁷³ E. Chapon,¹⁵ G. Chen,⁵³ S.W. Cho,²⁷ S. Choi,²⁷ B. Choudhary,²⁴ S. Cihangir[‡],⁴⁵ D. Claes,⁵⁹ J. Clutter,⁵³ M. Cooke^k,⁴⁵ W.E. Cooper,⁴⁵ M. Corcoran,⁷³ F. Couderc,¹⁵ M.-C. Cousinou,¹² J. Cuth,²¹ D. Cutts,⁷⁰ A. Das,⁷² G. Davies,⁴⁰ S.J. de Jong,^{29,30} E. De La Cruz-Burelo,²⁸ F. Déliot,¹⁵ R. Demina,⁶³ D. Denisov,⁴⁵ S.P. Denisov,³⁴ S. Desai,⁴⁵ C. Deterre^c,⁴¹ K. DeVaughan,⁵⁹ H.T. Diehl,⁴⁵ M. Diesburg,⁴⁵ P.F. Ding,⁴¹ A. Dominguez,⁵⁹ A. Drutskoy^p,³² A. Dubey,²⁴ L.V. Dudko,³³ A. Duperrin,¹² S. Dutt,²³ M. Eads,⁴⁷ D. Edmunds,⁵⁷ J. Ellison,⁴³ V.D. Elvira,⁴⁵ Y. Enari,¹⁴ H. Evans,⁴⁹ A. Evdokimov,⁴⁶ V.N. Evdokimov,³⁴ A. Fauré,¹⁵ L. Feng,⁴⁷ T. Ferbel,⁶³ F. Fiedler,²¹ F. Filthaut,^{29,30} W. Fisher,⁵⁷ H.E. Fisk,⁴⁵ M. Fortner,⁴⁷ H. Fox,³⁹ J. Franc,⁷ S. Fuess,⁴⁵ P.H. Garbincius,⁴⁵ A. Garcia-Bellido,⁶³ J.A. García-González,²⁸ V. Gavrilov,³² W. Geng,^{12,57} C.E. Gerber,⁴⁶ Y. Gershtein,⁶⁰ G. Ginther,⁴⁵ O. Gogota,³⁸ G. Golovanov,³¹ P.D. Grannis,⁶⁴ S. Greder,¹⁶ H. Greenlee,⁴⁵ G. Grenier,¹⁷ Ph. Gris,¹⁰ J.-F. Grivaz,¹³ A. Grohsjean^c,¹⁵ S. Grünendahl,⁴⁵ M.W. Grünewald,²⁶ T. Guillemain,¹³ G. Gutierrez,⁴⁵ P. Gutierrez,⁶⁷ J. Haley,⁶⁸ L. Han,⁴ K. Harder,⁴¹ A. Harel,⁶³ J.M. Hauptman,⁵² J. Hays,⁴⁰ T. Head,⁴¹ T. Hebbeker,¹⁸ D. Hedin,⁴⁷ H. Hegab,⁶⁸ A.P. Heinson,⁴³ U. Heintz,⁷⁰ C. Hensel,¹ I. Heredia-De La Cruz^d,²⁸ K. Herner,⁴⁵ G. Hesketh^f,⁴¹ M.D. Hildreth,⁵¹ R. Hirosky,⁷⁴ T. Hoang,⁴⁴ J.D. Hobbs,⁶⁴ B. Hoeneisen,⁹ J. Hogan,⁷³ M. Hohlfeld,²¹ J.L. Holzbauer,⁵⁸ I. Howley,⁷¹ Z. Hubacek,^{7,15} V. Hynek,⁷ I. Iashvili,⁶² Y. Ilchenko,⁷² R. Illingworth,⁴⁵ A.S. Ito,⁴⁵ S. Jabeen^m,⁴⁵ M. Jaffré,¹³ A. Jayasinghe,⁶⁷ M.S. Jeong,²⁷ R. Jesik,⁴⁰ P. Jiang[‡],⁴ K. Johns,⁴² E. Johnson,⁵⁷ M. Johnson,⁴⁵ A. Jonckheere,⁴⁵ P. Jonsson,⁴⁰ J. Joshi,⁴³ A.W. Jung^o,⁴⁵ A. Juste,³⁶ E. Kajfasz,¹² D. Karmanov,³³ I. Katsanos,⁵⁹ M. Kaur,²³ R. Kehoe,⁷² S. Kermiche,¹² N. Khalatyan,⁴⁵ A. Khanov,⁶⁸ A. Kharchilava,⁶² Y.N. Khazdhar,³¹ I. Kiselevich,³² J.M. Kohli,²³ A.V. Kozelov,³⁴ J. Kraus,⁵⁸ A. Kumar,⁶² A. Kupco,⁸ T. Kurča,¹⁷ V.A. Kuzmin,³³ S. Lammers,⁴⁹ P. Lebrun,¹⁷ H.S. Lee,²⁷ S.W. Lee,⁵² W.M. Lee,⁴⁵ X. Lei,⁴² J. Lellouch,¹⁴ D. Li,¹⁴ H. Li,⁷⁴ L. Li,⁴³ Q.Z. Li,⁴⁵ J.K. Lim,²⁷ D. Lincoln,⁴⁵ J. Linnemann,⁵⁷ V.V. Lipaev[‡],³⁴ R. Lipton,⁴⁵ H. Liu,⁷² Y. Liu,⁴ A. Lobodenko,³⁵ M. Lokačicek,⁸ R. Lopes de Sa,⁴⁵ R. Luna-Garcia^g,²⁸ A.L. Lyon,⁴⁵ A.K.A. Maciel,¹ R. Madar,¹⁹ R. Magaña-Villalba,²⁸ S. Malik,⁵⁹ V.L. Malyshev,³¹ J. Mansour,²⁰ J. Martínez-Ortega,²⁸ R. McCarthy,⁶⁴ C.L. McGivern,⁴¹ M.M. Meijer,^{29,30} A. Melnitchouk,⁴⁵ D. Menezes,⁴⁷ P.G. Mercadante,³ M. Merkin,³³ A. Meyer,¹⁸ J. Meyerⁱ,²⁰ F. Miconi,¹⁶ N.K. Mondal,²⁵ M. Mulhearn,⁷⁴ E. Nagy,¹² M. Narain,⁷⁰ R. Nayyar,⁴² H.A. Neal,⁵⁶ J.P. Negret,⁵ P. Neustroev,³⁵ H.T. Nguyen,⁷⁴ T. Nunnemann,²² J. Orduna,⁷⁰ N. Osman,¹² A. Pal,⁷¹ N. Parashar,⁵⁰ V. Parihar,⁷⁰ S.K. Park,²⁷ R. Partridge^e,⁷⁰ N. Parua,⁴⁹ A. Patwa^j,⁶⁵ B. Penning,⁴⁰ M. Perfilov,³³ Y. Peters,⁴¹ K. Petridis,⁴¹ G. Petrillo,⁶³ P. Pétroff,¹³ M.-A. Pleier,⁶⁵ V.M. Podstavkov,⁴⁵ A.V. Popov,³⁴ M. Prewitt,⁷³ D. Price,⁴¹ N. Prokopenko,³⁴ J. Qian,⁵⁶ A. Quadt,²⁰ B. Quinn,⁵⁸ P.N. Ratoff,³⁹ I. Razumov,³⁴ I. Ripp-Baudot,¹⁶ F. Rizatdinova,⁶⁸ M. Rominsky,⁴⁵ A. Ross,³⁹ C. Royon,⁸ P. Rubinov,⁴⁵ R. Ruchti,⁵¹ G. Sajot,¹¹ A. Sánchez-Hernández,²⁸ M.P. Sanders,²² A.S. Santos^h,¹ G. Savage,⁴⁵ M. Savitskiy,³⁸ L. Sawyer,⁵⁴ T. Scanlon,⁴⁰ R.D. Schamberger,⁶⁴ Y. Scheglov,³⁵ H. Schellman,^{69,48} M. Schott,²¹ C. Schwanenberger,⁴¹ R. Schwienhorst,⁵⁷ J. Sekaric,⁵³ H. Severini,⁶⁷ E. Shabalina,²⁰ V. Shary,¹⁵ S. Shaw,⁴¹ A.A. Shchukin,³⁴ V. Simak,⁷ P. Skubic,⁶⁷ P. Slattery,⁶³ G.R. Snow,⁵⁹ J. Snow,⁶⁶ S. Snyder,⁶⁵ S. Söldner-Rembold,⁴¹ L. Sonnenschein,¹⁸ K. Soustruznik,⁶ J. Stark,¹¹ N. Stefaniuk,³⁸ D.A. Stoyanova,³⁴ M. Strauss,⁶⁷ L. Suter,⁴¹ P. Svoisky,⁷⁴ M. Titov,¹⁵ V.V. Tokmenin,³¹ Y.-T. Tsai,⁶³ D. Tsybychev,⁶⁴ B. Tuchming,¹⁵ C. Tully,⁶¹ L. Uvarov,³⁵ S. Uvarov,³⁵ S. Uzunyan,⁴⁷ R. Van Kooten,⁴⁹ W.M. van Leeuwen,²⁹ N. Varelas,⁴⁶ E.W. Varnes,⁴² I.A. Vasilyev,³⁴ A.Y. Verkhnev,³¹ L.S. Vertogradov,³¹ M. Verzocchi,⁴⁵ M. Vesterinen,⁴¹ D. Vilanova,¹⁵ P. Vokac,⁷ H.D. Wahl,⁴⁴ M.H.L.S. Wang,⁴⁵ J. Warchol,⁵¹ G. Watts,⁷⁵ M. Wayne,⁵¹ J. Weichert,²¹ L. Welty-Rieger,⁴⁸ M.R.J. Williamsⁿ,⁴⁹ G.W. Wilson,⁵³ M. Wobisch,⁵⁴ D.R. Wood,⁵⁵ T.R. Wyatt,⁴¹ Y. Xie,⁴⁵ R. Yamada,⁴⁵ S. Yang,⁴ T. Yasuda,⁴⁵ Y.A. Yatsunenko,³¹ W. Ye,⁶⁴ Z. Ye,⁴⁵ H. Yin,⁴⁵ K. Yip,⁶⁵ S.W. Youn,⁴⁵ J.M. Yu,⁵⁶ J. Zennamo,⁶² T.G. Zhao,⁴¹ B. Zhou,⁵⁶ J. Zhu,⁵⁶ M. Zielinski,⁶³ D. Zieminska,⁴⁹ and L. Zivkovic¹⁴

(The D0 Collaboration*)

- ¹LAFEX, Centro Brasileiro de Pesquisas Físicas, Rio de Janeiro, RJ 22290, Brazil
²Universidade do Estado do Rio de Janeiro, Rio de Janeiro, RJ 20550, Brazil
³Universidade Federal do ABC, Santo André, SP 09210, Brazil
⁴University of Science and Technology of China, Hefei 230026, People's Republic of China
⁵Universidad de los Andes, Bogotá, 111711, Colombia
⁶Charles University, Faculty of Mathematics and Physics,
Center for Particle Physics, 116 36 Prague 1, Czech Republic
⁷Czech Technical University in Prague, 116 36 Prague 6, Czech Republic
⁸Institute of Physics, Academy of Sciences of the Czech Republic, 182 21 Prague, Czech Republic
⁹Universidad San Francisco de Quito, Quito, Ecuador
¹⁰LPC, Université Blaise Pascal, CNRS/IN2P3, Clermont, F-63178 Aubière Cedex, France
¹¹LPSC, Université Joseph Fourier Grenoble 1, CNRS/IN2P3,
Institut National Polytechnique de Grenoble, F-38026 Grenoble Cedex, France
¹²CPPM, Aix-Marseille Université, CNRS/IN2P3, F-13288 Marseille Cedex 09, France
¹³LAL, Univ. Paris-Sud, CNRS/IN2P3, Université Paris-Saclay, F-91898 Orsay Cedex, France
¹⁴LPNHE, Universités Paris VI and VII, CNRS/IN2P3, F-75005 Paris, France
¹⁵CEA Saclay, Irfu, SPP, F-91191 Gif-Sur-Yvette Cedex, France
¹⁶IPHC, Université de Strasbourg, CNRS/IN2P3, F-67037 Strasbourg, France
¹⁷IPNL, Université Lyon 1, CNRS/IN2P3, F-69622 Villeurbanne Cedex,
France and Université de Lyon, F-69361 Lyon CEDEX 07, France
¹⁸III. Physikalisches Institut A, RWTH Aachen University, 52056 Aachen, Germany
¹⁹Physikalisches Institut, Universität Freiburg, 79085 Freiburg, Germany
²⁰II. Physikalisches Institut, Georg-August-Universität Göttingen, 37073 Göttingen, Germany
²¹Institut für Physik, Universität Mainz, 55099 Mainz, Germany
²²Ludwig-Maximilians-Universität München, 80539 München, Germany
²³Panjab University, Chandigarh 160014, India
²⁴Delhi University, Delhi-110 007, India
²⁵Tata Institute of Fundamental Research, Mumbai-400 005, India
²⁶University College Dublin, Dublin 4, Ireland
²⁷Korea Detector Laboratory, Korea University, Seoul, 02841, Korea
²⁸CINVESTAV, Mexico City 07360, Mexico
²⁹Nikhef, Science Park, 1098 XG Amsterdam, the Netherlands
³⁰Radboud University Nijmegen, 6525 AJ Nijmegen, the Netherlands
³¹Joint Institute for Nuclear Research, Dubna 141980, Russia
³²Institute for Theoretical and Experimental Physics, Moscow 117259, Russia
³³Moscow State University, Moscow 119991, Russia
³⁴Institute for High Energy Physics, Protvino, Moscow region 142281, Russia
³⁵Petersburg Nuclear Physics Institute, St. Petersburg 188300, Russia
³⁶Institució Catalana de Recerca i Estudis Avançats (ICREA) and Institut
de Física d'Altes Energies (IFAE), 08193 Bellaterra (Barcelona), Spain
³⁷Uppsala University, 751 05 Uppsala, Sweden
³⁸Taras Shevchenko National University of Kyiv, Kiev, 01601, Ukraine
³⁹Lancaster University, Lancaster LA1 4YB, United Kingdom
⁴⁰Imperial College London, London SW7 2AZ, United Kingdom
⁴¹The University of Manchester, Manchester M13 9PL, United Kingdom
⁴²University of Arizona, Tucson, Arizona 85721, USA
⁴³University of California Riverside, Riverside, California 92521, USA
⁴⁴Florida State University, Tallahassee, Florida 32306, USA
⁴⁵Fermi National Accelerator Laboratory, Batavia, Illinois 60510, USA
⁴⁶University of Illinois at Chicago, Chicago, Illinois 60607, USA
⁴⁷Northern Illinois University, DeKalb, Illinois 60115, USA
⁴⁸Northwestern University, Evanston, Illinois 60208, USA
⁴⁹Indiana University, Bloomington, Indiana 47405, USA
⁵⁰Purdue University Calumet, Hammond, Indiana 46323, USA
⁵¹University of Notre Dame, Notre Dame, Indiana 46556, USA
⁵²Iowa State University, Ames, Iowa 50011, USA
⁵³University of Kansas, Lawrence, Kansas 66045, USA
⁵⁴Louisiana Tech University, Ruston, Louisiana 71272, USA
⁵⁵Northeastern University, Boston, Massachusetts 02115, USA
⁵⁶University of Michigan, Ann Arbor, Michigan 48109, USA
⁵⁷Michigan State University, East Lansing, Michigan 48824, USA
⁵⁸University of Mississippi, University, Mississippi 38677, USA

- ⁵⁹University of Nebraska, Lincoln, Nebraska 68588, USA
⁶⁰Rutgers University, Piscataway, New Jersey 08855, USA
⁶¹Princeton University, Princeton, New Jersey 08544, USA
⁶²State University of New York, Buffalo, New York 14260, USA
⁶³University of Rochester, Rochester, New York 14627, USA
⁶⁴State University of New York, Stony Brook, New York 11794, USA
⁶⁵Brookhaven National Laboratory, Upton, New York 11973, USA
⁶⁶Langston University, Langston, Oklahoma 73050, USA
⁶⁷University of Oklahoma, Norman, Oklahoma 73019, USA
⁶⁸Oklahoma State University, Stillwater, Oklahoma 74078, USA
⁶⁹Oregon State University, Corvallis, Oregon 97331, USA
⁷⁰Brown University, Providence, Rhode Island 02912, USA
⁷¹University of Texas, Arlington, Texas 76019, USA
⁷²Southern Methodist University, Dallas, Texas 75275, USA
⁷³Rice University, Houston, Texas 77005, USA
⁷⁴University of Virginia, Charlottesville, Virginia 22904, USA
⁷⁵University of Washington, Seattle, Washington 98195, USA
(Dated: February 4, 2018)

We report evidence for a narrow structure, $X(5568)$, in the decay sequence $X(5568) \rightarrow B_s^0 \pi^\pm$, $B_s^0 \rightarrow J/\psi \phi$, $J/\psi \rightarrow \mu^+ \mu^-$, $\phi \rightarrow K^+ K^-$. This is evidence for the first instance of a hadronic state with valence quarks of four different flavors. The mass and natural width of this state are measured to be $m = 5567.8 \pm 2.9$ (stat) $^{+0.9}_{-1.9}$ (syst) MeV/ c^2 and $\Gamma = 21.9 \pm 6.4$ (stat) $^{+5.0}_{-2.5}$ (syst) MeV/ c^2 . If the decay is $X(5568) \rightarrow B_s^* \pi^\pm \rightarrow B_s^0 \gamma \pi^\pm$ with an unseen γ , $m(X(5568))$ will be shifted up by $m(B_s^*) - m(B_s^0) \sim 49$ MeV/ c^2 . This measurement is based on 10.4 fb^{-1} of $p\bar{p}$ collision data at $\sqrt{s} = 1.96$ TeV collected by the D0 experiment at the Fermilab Tevatron collider.

PACS numbers: 14.40.Rt, 13.25.Gv, 12.39.Mk

During the last few years several resonant states that cannot be conventional quark-antiquark mesons or three-quark baryons have been observed [1–8]. Taking into account the decay modes and charges of these states, they may be interpreted as four-quark or five-quark states. These states have one common feature: they consist of a combination of heavy and light quarks. These discoveries open up a new era of multiquark hadron spectroscopy. Various combinations of heavy and light mesons may be tested. One such system is the combination of the heavy B_s^0 or \bar{B}_s^0 meson and the light π^\pm meson. Such systems are composed of two quarks and two antiquarks of four different flavors: b, s, u, d , which might be a tightly

bound diquark antidiquark pair such as $[bu][\bar{d}\bar{s}]$, $[bd][\bar{s}\bar{u}]$, $[su][\bar{b}\bar{d}]$, or $[sd][\bar{b}\bar{u}]$, or a “molecule” of the loosely bound B and K mesons. This Letter presents a study of the $B_s^0 \pi^\pm$ invariant mass spectrum using a data sample of 10.4 fb^{-1} collected with the D0 detector at the Fermilab Tevatron collider.

The D0 detector consists of a central tracking system, calorimeters, and muon detectors [9]. The central tracking system comprises a silicon microstrip tracker (SMT) and a central fiber tracker (CFT), both located inside a 1.9 T superconducting solenoidal magnet. The tracking system is designed to optimize tracking and vertexing for pseudorapidities $|\eta| < 3$, where $\eta = -\ln|\tan(\theta/2)|$, and θ is the polar angle with respect to the proton beam direction. The SMT can reconstruct the $p\bar{p}$ interaction vertex (primary vertex) for interactions with at least three tracks with a precision of $40 \mu\text{m}$ in the plane transverse to the beam direction. The muon detector, positioned outside the calorimeter, consists of a central muon system covering the pseudorapidity region $|\eta| < 1$ and a forward muon system covering the pseudorapidity region $1 < |\eta| < 2$. Both central and forward systems consist of a layer of drift tubes and scintillators inside 1.8 T iron toroidal magnets with two similar layers outside the toroids.

Events used in this analysis are collected with both single muon and dimuon triggers. Single muon triggers require a coincidence of signals in trigger elements inside and outside the toroidal magnets. Dimuon triggers in the central rapidity region require at least one muon to penetrate the toroid. In the forward region, both muons

*with visitors from ^aAugustana College, Sioux Falls, SD 57197, USA, ^bThe University of Liverpool, Liverpool L69 3BX, UK, ^cDeutsches Elektronen-Synchrotron (DESY), Notkestrasse 85, Germany, ^dCONACyT, M-03940 Mexico City, Mexico, ^eSLAC, Menlo Park, CA 94025, USA, ^fUniversity College London, London WC1E 6BT, UK, ^gCentro de Investigacion en Computacion - IPN, CP 07738 Mexico City, Mexico, ^hUniversidade Estadual Paulista, São Paulo, SP 01140, Brazil, ⁱKarlsruher Institut für Technologie (KIT) - Steinbuch Centre for Computing (SCC), D-76128 Karlsruhe, Germany, ^jOffice of Science, U.S. Department of Energy, Washington, D.C. 20585, USA, ^kAmerican Association for the Advancement of Science, Washington, D.C. 20005, USA, ^lKiev Institute for Nuclear Research (KINR), Kyiv 03680, Ukraine, ^mUniversity of Maryland, College Park, MD 20742, USA, ⁿEuropean Organization for Nuclear Research (CERN), CH-1211 Geneva, Switzerland, ^oPurdue University, West Lafayette, IN 47907, USA, and ^pLebedev Physical Institute of the Russian Academy of Sciences, Moscow, 119991, Russia. [†]Deceased.

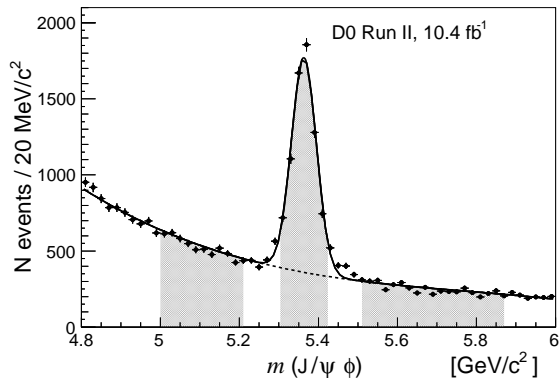


FIG. 1: Invariant mass distribution of $J/\psi\phi$ candidates. The signal region and two sideband regions are indicated. The solid curve presents the fit results to the function, modeled by a sum of a third-order polynomial to describe the combinatorial background and a Gaussian to describe the B_s^0 signal. The dotted curve shows the combinatorial background.

are required to penetrate the toroid.

Candidate events are required to include a pair of oppositely charged muons both with $p_T > 1.5$ GeV/ c in the invariant mass range $2.92 < m(\mu^+\mu^-) < 3.25$ GeV/ c^2 , consistent with J/ψ decay, accompanied by two additional particles of opposite charge assumed to be kaons, each with $p_T > 0.7$ GeV/ c , with an invariant mass of $1.012 < m(K^+K^-) < 1.030$ GeV/ c^2 , consistent with ϕ decay, and a third charged particle with $p_T > 0.5$ GeV/ c assumed to be a pion.

In the event selection, both muons are required to be detected in the muon chambers inside the toroidal magnet, and at least one of the muons is required to be also detected outside the iron toroid. Each muon candidate [10] is required to match a track found in the central tracking system, and each of the five final-state tracks is required to have at least one SMT hit and at least one CFT hit. The dimuon invariant mass is constrained to the world-average J/ψ mass [11], and the four tracks forming a $J/\psi\phi$ candidate are required to satisfy a fit to a common vertex that is displaced from the primary vertex in the plane perpendicular to the beam direction by at least 3 times the standard deviation of the measurement uncertainty. The pion candidate is required to be consistent with originating from the primary $p\bar{p}$ collision vertex.

To form a $B_s^0\pi^\pm$ combination, we select the B_s^0 candidates in the mass range $5.303 < m(J/\psi\phi) < 5.423$ GeV/ c^2 , corresponding to an interval of ± 2 standard deviations around the mean value of the reconstructed B_s^0 mass. The $m(J/\psi\phi)$ distribution is shown in Fig. 1. The fit, including a third-order polynomial describing the combinatorial background and a Gaussian function describing the signal, yields the Gaussian signal parameters $m(B_s^0) = 5363.3 \pm 0.6$ MeV/ c^2 , $\sigma(B_s^0) = 31.6 \pm 0.6$ MeV/ c^2 and the number of sig-

nal events $N_{\text{ev}} = 5582 \pm 100$. To improve the resolution of the invariant mass of the $B_s^0\pi^\pm$ system and to remove the measured B_s^0 mass bias, we define it as $m(B_s^0\pi^\pm) = m(J/\psi\phi\pi^\pm) - m(J/\psi\phi) + 5.3667$ GeV/ c^2 , where $m(J/\psi)$ is not constrained to the nominal value. We study events as a function of mass in the range $5.5 < m(J/\psi\phi) < 5.9$ GeV/ c^2 .

Background in the $B_s^0\pi^\pm$ invariant mass spectrum results from random combinations of selected B_s^0 candidates with low momentum charged particles coming mostly from the primary vertex. To suppress background the $B_s^0\pi^\pm$ system is required to have $p_T > 10$ GeV/ c . To further reduce background, we impose a limit on the difference between the directions of the B_s^0 candidate and the pion to be $\Delta R = \sqrt{\Delta\eta^2 + \Delta\phi^2} < 0.3$, where η is the pseudorapidity and ϕ is the azimuthal angle. In addition to increasing the signal-to-background ratio this ‘‘cone cut’’ limits backgrounds that are not included in available simulations.

The B_s^0 candidates include genuine B_s^0 mesons and the combinatorial background under the B_s^0 signal, as seen in Fig. 1. The $B_s^0\pi^\pm$ background with a real B_s^0 meson is modeled using a Monte Carlo (MC) simulation [12] of events containing a B_s^0 meson and additional pions tuned to reproduce the B_s^0 transverse momentum distribution in data.

The background with a false B_s^0 meson is modeled using the sideband events obtained from data. The chosen sideband regions $5.0 < m(J/\psi\phi) < 5.21$ GeV/ c^2 and $5.51 < m(J/\psi\phi) < 5.87$ GeV/ c^2 are indicated in Fig. 1. The sidebands are separated by $\sim 5\sigma$ from the B_s^0 nominal mass. The left and right sideband ranges are chosen to provide a large event sample and to have an average mass of $m(B_s^0)$.

The two background components are found to have similar shapes [13]. The fraction of the real B_s^0 events in the signal region is obtained from the fit to the B_s^0 meson in the $m(J/\psi\phi)$ distribution and is found to be $(70.9 \pm 0.6)\%$. MC events and the sideband events are mixed in this proportion to obtain the combined background that includes pions from both sources. The event selection results in pions that mainly come from the primary vertex, although pions originating from heavy flavor decays are also present in the sample.

Multiple entries for a single event may occur when more than one pion candidate passes the event selection and they are retained in the sample. The rate of duplicate entries in the mass range $5.5 < m(B_s^0\pi^\pm) < 5.6$ GeV/ c^2 ($\sim 5\%$) is lower than for masses above 5.7 GeV/ c^2 ($\sim 8\%$).

The combined background is modeled by a function of the parameter $m_0 = m_{B\pi} - \Delta$, where $m_{B\pi} \equiv m(B_s^0\pi^\pm)$ and $\Delta = 5.5$ GeV/ c^2 , of the form

$$F_{\text{bgr}}(m_0) = P_{4(C_1=0)} \exp(P_2). \quad (1)$$

Here, $P_{4(C_1=0)}$ and P_2 are fourth- and second-order polynomials, and the linear term of the first polynomial is set

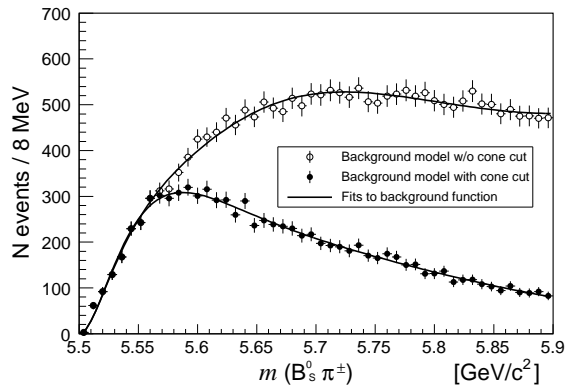


FIG. 2: The combined background for the $m(B_s^0\pi^\pm)$ distribution described in the text and the fit to that distribution with the $\Delta R < 0.3$ cone cut and without the cone cut.

to zero. This empirical function gives a good description of the combined backgrounds, as seen in Fig. 2.

The $B_s^0\pi^\pm$ invariant mass spectrum is shown in Fig. 3(a) with the cone cut and (b) without the cone cut. An enhancement is seen near $5.57 \text{ GeV}/c^2$. To extract the signal parameters, the distributions are fitted with a function F [Eq. (2)] that includes two terms: the background term $F_{\text{bgr}}(m_{B\pi})$ with fixed shape parameters as in Fig. 2 and the signal term $F_{\text{sig}}(m_{B\pi}, M_X, \Gamma_X)$, modeled by a relativistic Breit-Wigner function convolved with a Gaussian detector resolution function and with the mass-dependent efficiency of the cone cut [13]. Here M_X and Γ_X are the mass and the natural width of the resonance. The Gaussian width parameter $\sigma_{\text{res}} = 3.8 \text{ MeV}/c^2$ is taken from simulations.

The fit function has the form

$$F = f_{\text{sig}} F_{\text{sig}}(m_{B\pi}, M_X, \Gamma_X) + f_{\text{bgr}} F_{\text{bgr}}(m_{B\pi}), \quad (2)$$

where f_{sig} and f_{bgr} are normalization factors.

We use the Breit-Wigner parametrization appropriate for an S -wave two-body decay near threshold:

$$BW(m_{B\pi}) \propto \frac{M_X^2 \Gamma(m_{B\pi})}{(M_X^2 - m_{B\pi}^2)^2 + M_X^2 \Gamma^2(m_{B\pi})}. \quad (3)$$

The mass-dependent width $\Gamma(m_{B\pi}) = \Gamma_X \cdot (q_1/q_0)$ is proportional to the natural width Γ_X , where q_1 and q_0 are three-vector momenta of the B_s^0 meson in the rest frame of the $B_s^0\pi^\pm$ system at the invariant mass equal to $m_{B\pi}$ and M_X , respectively.

In the fit shown in Fig. 3(a), the normalization parameters f_{sig} and f_{bgr} and the Breit-Wigner parameters M_X and Γ_X are allowed to vary. The fit yields the mass and width of $M_X = 5567.8 \pm 2.9 \text{ MeV}/c^2$, $\Gamma_X = 21.9 \pm 6.4 \text{ MeV}/c^2$, and the number of signal events of $N = 133 \pm 31$. As the measured width is significantly larger than the experimental mass resolution, we infer

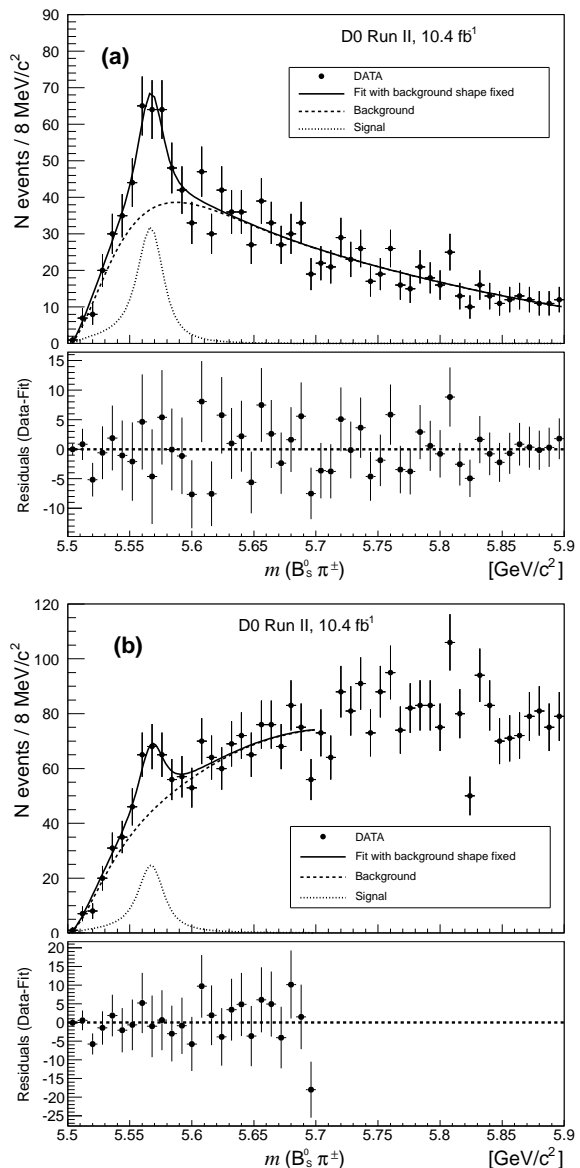


FIG. 3: The $m(B_s^0\pi^\pm)$ distribution together with the background distribution and the fit results (a) after applying the $\Delta R < 0.3$ cone cut and (b) without the cone cut.

that $X(5568) \rightarrow B_s^0\pi^\pm$ is a strong decay. The statistical significance of the signal is defined as $\sqrt{-2 \ln(\mathcal{L}_0/\mathcal{L}_{\text{max}})}$, where \mathcal{L}_{max} and \mathcal{L}_0 are likelihood values at the best-fit signal yield and the signal yield fixed to zero. The obtained local statistical significance is 6.6σ for the given mass and width values. With the look-elsewhere effect [14] taken into account, the global statistical significance is 6.1σ . The search window is taken as the interval between the $B_s^0\pi^\pm$ threshold ($5506 \text{ MeV}/c^2$) and the $B_d^0 K^\pm$ mass threshold ($5774 \text{ MeV}/c^2$).

We also extract the signal from the $m(B_s^0\pi^\pm)$ distribution without the ΔR cone cut, fixing the mass and natural width of the signal and the background mass shape to their default values. We see a tendency for data to

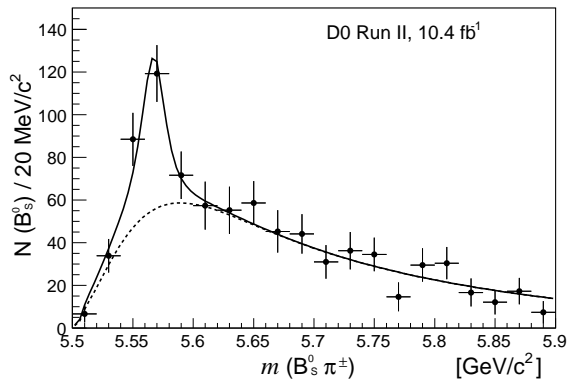


FIG. 4: The $m(B_s^0\pi^\pm)$ distribution resulting from fits of the B_s^0 signal to $m(J/\psi\phi)$ in twenty mass intervals of $(B_s^0\pi^\pm)$ candidates described in the text. The solid line shows the result of the fit. The dashed line shows the contribution of events due to the B_s^0 background from simulations. There is no non- B_s^0 background.

exceed background for $m(B_s^0\pi^\pm) > M_X$ [13]. We perform a fit in the restricted range $m(B_s^0\pi^\pm) < 5.7 \text{ GeV}/c^2$ [Fig. 3(b)] and find the fitted number of signal events to be 106 ± 23 , with a corresponding local statistical significance of 4.8σ . The difference in yields with and without the cone cut is not fully explained by statistical fluctuations. In a subsidiary study we used empirical functions [15] for the background fitted to the sidebands in data below the $X(5568)$ region and above the signal region up to $5.9 \text{ GeV}/c^2$ and found signal yields that are greater than those with the default background function and comparable to or greater than that found in the cone cut analysis. These results confirm that using a background function that agrees with data for masses above 5.7 GeV can increase the fitted signal yield above that obtained using the default background model. Additional background processes not present in our MC calculations such as $B_c \rightarrow B_s n\pi$ with $n > 1$, or other new states at higher mass, would thus have the effect of reducing the $X(5568)$ yield for the no-cone cut case.

As a cross-check, we extract a pure $B_s^0\pi^\pm$ signal by performing fits of the number of B_s^0 events in the $J/\psi\phi$ mass distribution in $20 \text{ MeV}/c^2$ intervals in the range $5.5 < m(B_s^0\pi^\pm) < 5.9 \text{ MeV}/c^2$. Results of those fits are shown in Fig. 4. A fit to the dependence of resulting B_s^0 yields on $m(B_s^0\pi^\pm)$, with the mass and natural width fixed to the previously obtained values, gives 118 ± 22 signal events. This result confirms that the observed signal is due to $B_s^0\pi^\pm$ candidates with genuine B_s^0 mesons and thus eliminates the possibility of non- B_s^0 processes mimicking the signal.

We obtain the systematic uncertainties for the measured values of the $X(5568)$ state mass, natural width, and the number of events. The dominant uncertainties are due to the background and signal shapes. We evaluate the systematic uncertainties due to the background

shape by (i) using different models of bottom pair production in generating the B_s^0 MC samples, (ii) varying the sideband mass intervals, (iii) changing the way the B_s^0 mass constraint is applied in the calculation of $m(B_s^0\pi^\pm)$ for the sideband events by replacing the mass difference defined in the text by the kinetic energy obtained by forcing $m(J/\psi\phi)$ to the world-average B_s^0 mass, (iv) changing the ratio of the MC to the sideband events within 1σ , (v) using different background functions by replacing the fourth-order polynomial in Eq. (1) with a third- or fifth-order polynomial or replacing the second-order polynomial in the exponential with the first- or third-order polynomial, and (vi) varying the nominal B_s^0 mass within $\pm 1 \text{ MeV}/c^2$ in the background samples, both for the sideband data and simulated events. The systematic uncertainties due to the signal shape are evaluated by (i) varying the detector resolution within $\pm 1 \text{ MeV}/c^2$ around the mean value, (ii) using a nonrelativistic Breit-Wigner function, and (iii) using a P -wave relativistic Breit-Wigner function.

Additionally, we estimate the systematic uncertainties due to the binning by changing the bin size to $5 \text{ MeV}/c^2$, and to $10 \text{ MeV}/c^2$ instead of $8 \text{ MeV}/c^2$, and shifting the lower edge of the mass scale by $1/3$, $1/2$, and $2/3$ of the bin size. All systematic uncertainty sources are summarized in Table 1. The uncertainties are added in quadrature separately for positive and negative values to obtain the total systematic uncertainties for each measured parameter and are treated as nuisance parameters to construct a prior predictive model [11, 16] of our test statistic. When the systematic uncertainties are included, the significance of the observed signal, including the look-elsewhere effect, is reduced to 5.1σ . For the analysis without the ΔR cut [Fig. 3(b)] we obtain a significance including the systematic uncertainty and the look-elsewhere effect of 3.9σ .

The stability of the result is checked by examining subsamples with (i) different signs of the π^\pm meson, (ii) different ranges of the azimuth and rapidity, (iii) the distance between the B_s^0 vertex and the primary vertex changed to five standard deviations, (iv) different B_s^0 mass windows (1.7σ , 1.5σ , 1.2σ), (v) different $B_s^0\pi^\pm$ momentum intervals ($p_T > 9 \text{ GeV}/c$, $p_T > 12 \text{ GeV}/c$), and (vi) different cone cuts ($\Delta R < 0.2$, $\Delta R < 0.15$). Taking into account the efficiencies of these cuts, no unexpected behaviors are observed in these tests.

The invariant mass spectra of B_s^0 candidates and charged tracks with kaon or proton mass hypotheses, are checked and no resonantlike enhancements in these distributions are found.

We measure the ratio ρ of the yield of the new state $X(5568)$ to the yield of the B_s^0 meson in two kinematic ranges, $10 < p_T(B_s^0) < 15 \text{ GeV}/c$ and $15 < p_T(B_s^0) < 30 \text{ GeV}/c$, by repeating the $m(B_s^0\pi)$ fits with free mass and width parameters for the $X(5568)$ signal [13]. The results for ρ are $(9.1 \pm 2.6 \pm 1.6)\%$ and $(8.2 \pm 2.7 \pm 1.6)\%$, respectively, with an average of $(8.6 \pm 1.9 \pm 1.4)\%$. The systematic uncertainties due to B_s^0 reconstruction effi-

TABLE I: Systematic uncertainties for the observed $X(5568)$ state mass, natural width and number of events.

Source	Mass, MeV/ c^2	Width, MeV/ c^2	Rate, %
<i>Background shape</i>			
MC samples with soft or hard B_s^0	+0.2 ; -0.6	+2.6 ; -0.0	+8.2 ; -0.0
Sideband mass ranges	+0.2 ; -0.1	+0.7 ; -1.7	+1.6 ; -9.3
Sideband mass calculation method	+0.1 ; -0.0	+0.0 ; -0.4	+0.0 ; -1.3
MC to sideband events ratio	+0.1 ; -0.1	+0.5 ; -0.6	+2.8 ; -3.1
Background function used	+0.5 ; -0.5	+0.1 ; -0.0	+0.2 ; -1.1
B_s^0 mass scale, MC and data	+0.1 ; -0.1	+0.7 ; -0.6	+3.4 ; -3.6
<i>Signal shape</i>			
Detector resolution	+0.1 ; -0.1	+1.5 ; -1.5	+2.1 ; -1.7
Non-relativistic BW	+0.0 ; -1.1	+0.3 ; -0.0	+3.1 ; -0.9
P -wave BW	+0.0 ; -0.6	+3.1 ; -0.0	+3.8 ; -0.0
<i>Other</i>			
Binning	+0.6 ; -1.1	+2.3 ; -0.0	+3.5 ; -3.3
Total	+0.9 ; -1.9	+5.0 ; -2.5	+11.4 ; -11.2

ciency cancel out in the ratio. The combined factor of the soft pion kinematic acceptance, reconstruction efficiency, and selection efficiency is obtained from a simulated samples of events with a spinless particle of mass equal to 5568 MeV/ c^2 decaying to B_s^0 and a charged pion. The pion efficiency increases with $p_T(B_s^0)$ from $(26.1 \pm 3.2)\%$ to $(42.1 \pm 6.5)\%$ for the two $p_T(B_s^0)$ ranges. The systematic uncertainty due to a potential difference of the soft pion reconstruction efficiency in MC calculations and data of $\pm 5\%$ is accounted for in systematics. Within uncertainties, the production ratio ρ does not depend on $p_T(B_s^0)$.

A possible interpretation of the observed structure is a four-quark state made up of a diquark-antidiquark pair. With the $B_s^0\pi^+$ produced in an S -wave, its quantum numbers would be $J^P = 0^+$. Thus, the state may be a heavy analog of the isotriplet scalar state $a(980)$, with an s quark replaced by a b quark. Such open charm and open bottom scalar mesons are predicted in Ref. [17]. On the other hand, the state can decay through the chain $B_s^*\pi^\pm$, $B_s^* \rightarrow B_s^0\gamma$, where the low-energy photon is not detected. In this case, the quantum numbers of this state would be $J^P = 1^+$, which would make it a counterpart to other heavy tetraquark candidates. The mass of the new state would be shifted by addition of the nominal mass difference $m(B_s^*) - m(B_s^0)$, while its width would remain unchanged. The large difference between the mass of this state and the sum of the B_d and K^\pm masses implies [18] that $X(5568)$ is unlikely to be a molecular state composed of loosely bound B_d and K^\pm mesons.

In summary, a structure is seen in the $B_s^0\pi^\pm$ invariant mass spectrum near threshold with a statistical significance, including the look-elsewhere effect, of 6.1σ . When the systematic uncertainties are included, the significance of the signal is 5.1σ . For the alternate analysis without the ΔR cut, we find the corresponding signif-

icance of 3.9σ . This structure may be interpreted as a tetraquark state with four different valence quark flavors, b, s, u, d . The mass and natural width of the $X(5568)$ state are $m = 5567.8 \pm 2.9$ (stat) $_{-1.9}^{+0.9}$ (syst) MeV/ c^2 and $\Gamma = 21.9 \pm 6.4$ (stat) $_{-2.5}^{+5.0}$ (syst) MeV/ c^2 .

We thank E. Gross and O. Vittels for useful discussions. We thank the staff at Fermilab and collaborating institutions, and acknowledge support from the Department of Energy and National Science Foundation (United States of America); Alternative Energies and Atomic Energy Commission and National Center for Scientific Research/National Institute of Nuclear and Particle Physics (France); Ministry of Education and Science of the Russian Federation, National Research Center ‘‘Kurchatov Institute’’ of the Russian Federation, and Russian Foundation for Basic Research (Russia); National Council for the Development of Science and Technology and Carlos Chagas Filho Foundation for the Support of Research in the State of Rio de Janeiro (Brazil); Department of Atomic Energy and Department of Science and Technology (India); Administrative Department of Science, Technology and Innovation (Colombia); National Council of Science and Technology (Mexico); National Research Foundation of Korea (Korea); Foundation for Fundamental Research on Matter (Netherlands); Science and Technology Facilities Council and The Royal Society (United Kingdom); Ministry of Education, Youth and Sports (Czech Republic); Bundesministerium für Bildung und Forschung (Federal Ministry of Education and Research) and Deutsche Forschungsgemeinschaft (German Research Foundation) (Germany); Science Foundation Ireland (Ireland); Swedish Research Council (Sweden); China Academy of Sciences and National Natural Science Foundation of China (China); and Ministry of Education and Science of Ukraine (Ukraine).

[1] S.-K. Choi *et al.* (Belle Collaboration), Observation of a Resonancelike Structure in the $\pi^\pm\psi'$ Mass Distribution

in Exclusive $B \rightarrow K\pi^\pm\psi'$ Decays, Phys. Rev. Lett. **100**,

- 142001 (2008).
- [2] R. Mizuk *et al.* (Belle Collaboration), Observation of two resonancelike structures in the $\pi^+\chi_{c1}$ mass distribution in exclusive $\overline{B}^0 \rightarrow K^-\pi^+\chi_{c1}$ decays, Phys. Rev. D **78**, 072004 (2008).
- [3] T. Aaltonen *et al.* (CDF Collaboration), Evidence for a Narrow Near-Threshold Structure in the $J/\psi\phi$ Mass Spectrum in $B^+ \rightarrow J/\psi\phi K^+$ Decays, Phys. Rev. Lett. **102**, 242002 (2009).
- [4] A. Bondar *et al.* (Belle Collaboration), Observation of Two Charged Bottomoniumlike Resonances in $\Upsilon(5S)$ Decays, Phys. Rev. Lett. **108**, 122001 (2012).
- [5] M. Ablikim *et al.* (BESIII Collaboration), Observation of a Charged Charmoniumlike Structure in $e^+e^- \rightarrow \pi^+\pi^-J/\psi$ at $\sqrt{s} = 4.26$ GeV, Phys. Rev. Lett. **110**, 252001 (2013).
- [6] Z. Q. Liu *et al.* (Belle Collaboration), Study of $e^+e^- \rightarrow \pi^+\pi^-J/\psi$ and Observation of a Charged Charmoniumlike State at Belle, Phys. Rev. Lett. **110**, 252002 (2013).
- [7] M. Ablikim *et al.* (BESIII Collaboration), Observation of a Charged Charmoniumlike Structure in $e^+e^- \rightarrow (D^*\overline{D}^{*\pm})\pi^\mp$ at $\sqrt{s} = 4.26$ GeV, Phys. Rev. Lett. **112**, 132001 (2014).
- [8] R. Aaij *et al.* (LHCb Collaboration), Observation of $J/\psi p$ Resonances Consistent with Pentaquark States in $\Lambda_b^0 \rightarrow J/\psi K^- p$ Decays, Phys. Rev. Lett. **115**, 072001 (2015).
- [9] V. M. Abazov *et al.* (D0 Collaboration), The upgraded D0 detector, Nucl. Instrum. Methods Phys. Res., Sect. A **565**, 463 (2006).
- [10] V. M. Abazov *et al.* (D0 Collaboration), Muon reconstruction and identification with the Run II D0 detector, Nucl. Instrum. Methods Phys. Res., Sect. A **737**, 281 (2014).
- [11] K. A. Olive *et al.*, (Particle Data Group), Review of particle physics, Chin. Phys. C **38**, 090001 (2014).
- [12] T. Sjöstrand *et al.*, High-energy-physics event generation with PYTHIA 6.1, Comput. Phys. Commun. **135**, 238 (2001). We use versions 6.323 and 6.409.
- [13] See Supplemental Material at <http://link.aps.org/supplemental/10.1103/PhysRevLett.000.000000> for brief description.
- [14] E. Gross and O. Vitells, Trial factors for the look elsewhere effect in high energy physics, Eur. Phys. J. **C70**, 525 (2010).
- [15] One alternate background function is a third order Chebychev polynomial. The second is that employed in a previous study of exotic heavy flavor mesons, V. M. Abazov *et al.* (D0 Collaboration), Inclusive Production of the $X(4140)$ State in $p\overline{p}$ Collisions at D0, Phys. Rev. Lett. **115**, 232001 (2015).
- [16] C. Giunti, Treatment of the background error in the statistical analysis of Poisson processes, Phys. Rev. D **59**, 113009 (1999).
- [17] L. Maiani, F. Piccinini, A. D. Polosa, and V. Riquer, New Look at Scalar Mesons, Phys. Rev. Lett. **93**, 212002 (2004).
- [18] M. Karliner, Doubly heavy tetraquarks and baryons, EPJ Web Conference **71**, 00065 (2014).